Journal of Bone Oncology 3 (2014) 67–76

Contents lists available at ScienceDirect

Journal of Bone Oncology

journal homepage: www.elsevier.com/locate/jbo

Research Paper

The SK-N-AS human neuroblastoma cell line develops osteolytic bone metastases with increased angiogenesis and COX-2 expression

Takahiro Tsutsumimoto [a,b], Paul Williams [a], Toshiyuki Yoneda [a,b,*]

[a] Division of Endocrinology and Metabolism, Department of Medicine, University of Texas Health Science Center at San Antonio, San Antonio, TX 78229-3900, USA

[b] Department of Cellular and Molecular Biochemistry, Osaka University Graduate School of Dentistry, Suita, Osaka 565-0871, Japan

ARTICLE INFO

Article history:
Received 30 September 2014
Accepted 3 October 2014
Available online 31 October 2014

Keywords:
Osteoclasts
Receptor activator of NF-κB ligand
Vascular endothelial growth factor-A
Microvessel density
Adrenal gland
COX-2 inhibitor

ABSTRACT

Neuroblastoma (NB), which arises from embryonic neural crest cells, is the most common extra-cranial solid tumor of childhood. Approximately half of NB patients manifest bone metastasis accompanied with bone pain, fractures and bone marrow failure, leading to disturbed quality of life and poor survival. To study the mechanism of bone metastasis of NB, we established an animal model in which intracardiac inoculation of the SK-N-AS human NB cells in nude mice developed osteolytic bone metastases with increased osteoclastogenesis. SK-N-AS cells induced the expression of receptor activator of NF-κB ligand and osteoclastogenesis in mouse bone marrow cells in the co-culture. SK-N-AS cells expressed COX-2 mRNA and produced substantial amounts of prostaglandin E_2 (PGE_2). In contrast, the SK-N-DZ and SK-N-FI human NB cells failed to develop bone metastases, induce osteoclastogenesis, express COX-2 mRNA and produce PGE_2. Immunohistochemical examination of SK-N-AS bone metastasis and subcutaneous tumor showed strong expression of COX-2. The selective COX-2 inhibitor NS-398 inhibited PGE_2 production and suppressed bone metastases with reduced osteoclastogenesis. NS-398 also inhibited subcutaneous SK-N-AS tumor development with decreased angiogenesis and vascular endothelial growth factor-A expression. Of interest, metastasis to the adrenal gland, a preferential site for NB development, was also diminished by NS-398. Our results suggest that COX2/PGE_2 axis plays a critical role in the pathophysiology of osteolytic bone metastases and tumor development of the SK-NS-AS human NB. Inhibition of angiogenesis by suppressing COX-2/PGE_2 may be an effective therapeutic approach for children with NB.

1. Introduction

Neuroblastoma (NB), which arises from embryonal neural crest cells, is the most common extra-cranial solid tumor of childhood and accounts for more than 15% of all child cancer death [1,2]. Patients with NB frequently manifest disseminated disease at first visit and prognosis of these patients is poor with 3-year survival rate less than 40% [1,2]. It has been well-known that bone is one of the most common target sites of NB spread. More than 60% of advanced NB patients manifest bone metastases that are radiologically osteolytic or a mixture of osteolytic and osteoblastic type [3,4]. Children with bone metastases suffer from complications including intolerable bone pain, pathological fractures and bone marrow failure. Currently-available anti-NB therapies are not satisfactorily effective at treating bone metastases and these complications. Accordingly, these children show miserable clinical courses and poor survival rate [5,6]. Therefore, control of bone metastases is an important goal in the management of infants with NB [7] and effective therapeutic interventions designed based on the understanding of the pathophysiology of bone metastasis of NB have been awaited. However, the mechanism underlying the preferential metastasis of NB to bone remains poorly understood.

Recent studies suggest that the interactions between cancer cells and bone microenvironment are critical to the pathophysiology of bone metastasis [8,9]. Bone provides a fertile soil for metastatic cancer cells by releasing growth factors such as insulin-like growth factors (IGFs) [10] and transforming growth factor β (TGFβ) [11] as a consequence of osteoclastic bone resorption during bone remodeling. Cancer cells stimulated by these bone-derived growth factors consequently produce increased levels of osteoclast-stimulating factors such as parathyroid hormone-related protein (PTH-rP) [11] and prostaglandin E_2 (PGE_2) [12], which in turn further promotes osteoclastic bone resorption, establishing a vicious cycle between bone-resorbing

* Corresponding author at: Division of Hematology/Oncology, Department of Medicine, Indiana University School of Medicine, Walther Hall R3-C321D, 980W. Walnut Street, Indianapolis, IN 46202, USA. Tel.: +1 317 274 6530; fax: +1 317 274 0396.
E-mail address: toshyone@iu.edu (T. Yoneda).

http://dx.doi.org/10.1016/j.jbo.2014.10.002

osteoclasts and metastatic cancer cells [8,9]. Contribution of similar vicious cycle between NB and bone microenvironment [13] mediated by receptor activator of NF-κB ligand (RANKL) [14,15] and IGF-1 [16] to the development and progression of NB bone metastasis has been also suggested.

In the present study, we developed an animal model of NB bone metastasis to advance our understanding of the mechanism of bone metastasis. We showed that an inoculation of the SK-N-AS human NB cells into the left heart ventricle of nude mice caused osteolytic bone metastases with increased osteoclastogenesis. SK-N-AS cells expressed COX-2 mRNA and produced substantial amounts of PGE_2. The selective COX-2 inhibitor NS-398 inhibited PGE_2 production and osteolytic bone metastases with reduced osteoclastic bone resorption and subcutaneous SK-N-AS tumor enlargement with reduced angiogenesis. These results suggest that COX-2/PGE_2 system plays a critical role in the pathophysiology of osteolytic bone metastases and tumor progression of NB. Inhibition of COX-2/PGE_2 is a potential therapeutic intervention for bone metastases in children with NB.

2. Materials and methods

2.1. Reagents and antibodies

Recombinant human osteoprotegerin (OPG) was purchased from BioSource International (Camarillo, CA). 1,25-dihydroxyvitamin D_3 ($1,25D_3$) was from BIOMOL International (Plymouth Meeting, PA). Dimethylsulfoxide (DMSO), PGE_2, and indomethacin were obtained from Sigma Chemical Co. (St. Louis, MO). NS-398, a selective COX-2 inhibitor, was purchased from Cayman Chemical Co. (Ann Arbor, MI). For *in vitro* use, indomethacin and NS-398 were reconstituted in DMSO and diluted with culture media. The final concentration of DMSO in the culture media was less than 0.1%.

Polyclonal rabbit anti-vascular endothelial growth factor-A (VEGF-A) and polyclonal rabbit anti-proliferation cell nuclear antigen (PCNA) were from Santa Cruz Biotechnology (Santa Cruz, CA). Polyclonal rabbit anti-COX-2 and polyclonal rabbit anti-factor VIII were from Zymed Laboratories, Inc. (South San Francisco, CA).

2.2. Human neuroblastoma cells

Human NB cell lines, SK-N-DZ, SK-N-AS, SK-N-FI, were obtained from American Type Culture Collection (Rockville, MD). All cells were maintained in Dulbecco's modified Eagle minimal essential medium (DMEM, Life Technologies, Inc., Grand Island, NY) supplemented with 10% fetal calf serum (FCS; Life Technologies, Inc.) at 37 °C under 5% CO_2 in air.

2.3. Tumorigenicity of human NB cell lines

Animal protocols were approved by the Institutional Animal Care and Use Committee at the University of Texas Health Science center at San Antonio and were in accordance with the NIH Guide for the Care and Use of Laboratory Animals. Animals were kept in our specific pathogen-free animal facilities. SK-N-DZ, SK-N-AS or SK-N-FI human NB cells (2.5×10^6) were suspended in 0.1 ml of phosphate buffered saline (PBS) and inoculated subcutaneously into the right flank of 4-week-old BALB/c-nu/nu (nude) mice (National Cancer Institute, Frederick, MD) (Day 0). Tumor volume was determined weekly based on the calculation suggested by the National Cancer Institute formula: Volume (cm^3)=(L cm × I^2 cm)/2, in which L is the largest diameter, and I is the smallest diameter of the tumor. Body weight (BW) of mice bearing with or without NB tumor was measured weekly until sacrifice. Subcutaneous (sc) tumors were excised and their wet weight was determined. A portion of the tumor tissue was fixed in 10% formalin for subsequent histological examinations and remaining tissues were snap-frozen in liquid nitrogen and stored at −80 °C for RNA extraction.

2.4. Bone metastases of human NB cell lines

Bone metastasis of SK-N-DZ, SK-N-AS or SK-N-FI human NB cells was studied using a well-characterized animal model we described previously [17]. Briefly, NB cells (5×10^5) were suspended in 0.1 ml of PBS and injected into the left heart ventricle of 4-week-old nude mice with 27-gauge needle under anesthesia with pentobarbital (0.05 mg/g body weight) (Day 0). Development of bone metastases was monitored weekly by X-ray. At 5 weeks, mice were euthanized and blood was collected for Ca^{2+} measurement and all bones and soft tissues were harvested and fixed in formalin for subsequent histological analyses.

2.5. Radiological monitoring of bone metastases

Animals were anesthetized deeply, then x-rayed in a prone position against the film (22 × 27 cm^2 X-Omat AR, Eastman Kodak Co., Rochester, NY) and exposed with X-rays at 35 KVP for 6 s using a Faxitron radiographic inspection unit (43855A; Faxitron X-ray Corporation, Buffalo Grove, IL) as described [17]. The radiographs were scanned and the area of osteolytic lesions was measured using NIH Image 1.62 and the results were expressed in square millimeters. The number of bone metastases was also counted in bilateral femurs and tibiae.

2.6. Ca^{2+} measurement

Ca^{2+} concentrations were measured in whole blood using a Ciba Corning 634 ISE Ca^{2+}/pH analyzer (Corning Medical and Scientific, Medfield, MA) and adjusted using the internal algorithm of the instrument to pH 7.4 as described previously [18].

2.7. Administration of a selective COX-2 inhibitor NS-398

Three days after the tumor cell inoculation, mice were divided into two groups, one group of mice received daily intraperitoneal (ip) injections of 100 μl vehicle (50% v/v DMSO) and another group of mice received NS-398 (15 mg/kg body weight) [12] until the end of the experiments.

2.8. Histology

Soft tissues and bones were removed from mice at the time of sacrifice, fixed in 10% buffered formalin for 2 days. Bones were further decalcified in 14% EDTA solution for 2 weeks at room temperature with gentle stirring. Subsequently, they were embedded in paraffin and stained with hematoxylin and eosin (H&E). Tartrate-resistant acid phosphatase (TRAP) staining was also performed according to the procedure described [12].

2.9. Immunohistochemistry

Paraffin sections (5 μm) were deparaffinized in xylene and rehydrated through graded alcohol [100%, 95%, 80% ethanol/double distilled H_2O (v/v)], and then rehydrated in PBS (pH 7.4). Sections were microwaved in 10 mM trisodium citrate (pH 6.0) for 4 min for antigen retrieval and then endogenous peroxidase activity was blocked by incubation in 3% H_2O_2/methanol for 30 min at room temperature. After a 30-min treatment with 10% normal goat serum diluted in PBS, sections were incubated

overnight at 4 °C with a 1:100–200 dilution of anti-VEGF-A, anti-PCNA, anti-COX-2 or anti-factor VIII antibody. Antibodies were diluted with PBS containing 1% normal goat serum. Normal rabbit IgG was used as negative control. The specimens were then rinsed and incubated with biotinylated anti-rabbit IgG (Vector Laboratories, Burlingame, CA) for 30 min at room temperature. Next, they were stained according to the avidin–biotin-peroxide complex (ABC) method using a commercial kit (Vectastain Elite ABC; Vector Laboratories). Subsequently, the specimens were counterstained with hematoxylin (VEGF-A, COX-2, and factor-VIII).

2.10. Co-cultures of human NB Cells and mouse bone marrow cells

Mouse bone marrow cells (BMCs) and spleen cells were isolated from 4- to 8-week-old male C57BL mice (Harlan, Indianapolis, IN) as described [19,20]. Briefly, femurs and tibiae were excised aseptically, cut off both ends. The marrow cavity of femurs and tibiae was flushed with α-minimum essential medium (αMEM, Life Technologies, Inc.) and then BMCs were collected. The collected BMCs (5×10^5 cells/48-well for TRAP stain, 4×10^6 cells/6-well for RNA extraction) were co-cultured with NB cells (0.5×10^4 cells/48-well for TRAP stain, 4×10^4 cells/6-well for RNA extraction) in αMEM containing 10% FCS in 48-well plates (0.2 ml/well) or 6-well plates (1.2 ml/well) for 6 days. As a positive control, BMCs were cultured in the presence of 10^{-8} M $1,25D_3$.

Spleen cells were obtained from splenic tissues aseptically collected from mice. NB cells (0.5×10^4 cells/well in a 48-well plate) were co-cultured with spleen cells (5×10^5 cells/well in a 48-well plate) in the presence or absence of bone marrow stromal cells (5×10^5 cells/well) for 8 days. The cultures were fed every 3 days by replacing a half of the spent medium with fresh medium. At the end of cultures, conditioned media were harvested and the cells adhering to the well surface were stained for TRAP using commercially available kits (Leukocyte acid phosphatase A kit, Sigma) or extracted RNA. TRAP-positive multinucleated cells (TRAP (+) MNCs) containing three or more nuclei per cell were counted as osteoclast-like cells (OC).

2.11. Prostaglandin E_2 (PGE_2) assay

Culture media were harvested at the end of experiments and frozen at −80 °C. Concentrations of PGE_2 in the culture media were determined using an EIA kit (Cayman Chemical Co.) according the protocol provided by the manufacture. Measurements were made in triplicate wells.

2.12. Reverse transcribed polymerase chain reaction (RT-PCR)

Total RNA was isolated using the TRI reagent (Sigma Chemical Co.) according to the manufacture's protocol. First-strand complementary DNAs (cDNAs) were synthesized from total RNA (1 μg) in 20 μl of reaction mixture containing oligo (dT) primer and superscript reverse transcriptase (Invitrogen, Carlsbad, CA). One microliter of this reaction was amplified using PCR primer sets for mouse RANKL [21], mouse OPG [21], mouse glyceraldehydes 3-phosphate dehydrogenase (GAPDH) [21], human COX-1 [22], human COX-2 [23], human VEGF-A [24], and human GAPDH [21] according to the manufacture's instruction (Invitrogen). The PCR products were analyzed by agarose gel electrophoresis and visualized by ethidium bromide staining under UV light.

2.13. Western analysis

After overnight serum starvation, cells were washed three times with ice-cold PBS, and lyzed in the lysis buffer [20 mM HEPES (pH 7.4), 150 mM NaCl, 1 mM EGTA, 1.5 mM $MgCl_2$, 10% glycerol, 1% Triton X-100, 10 μg/ml aprotinin, 10 μg/ml leupeptin, 1 mM PMSF, 0.1 mM sodium orthovanadate]. The cell lysates were boiled in SDS sample buffer containing 0.5 M beta-mercaptoethanol, separated by SDS-PAGE, transferred to nitrocellulose membranes and immunoblotted with anti-COX-2 antibody as described [12]. Separated proteins were visualized with horseradish peroxidase coupled with protein A (Kirkegaard & Perry laboratories, Inc., Gaithersburg, MD) with enhancement by chemiluminescence using ECL Western Blotting Detection Reagent (Amersham Bioscience Corp., Piscataway, NJ).

2.14. Statistical analysis

Results are expressed as the mean ± SE. Data were analyzed by either one-factor ANOVA followed by Turkey-Kramer post-hoc test, Mann-Whitney U test, or unpaired Student's t test. P values of < 0.05 were considered significant. All statistical analyses were carried out using Statview ver 5 (SAS Institute Inc., Berkeley, CA).

3. Results

3.1. Establishment of an animal model of bone metastasis of Human NB

Three human NB cell lines (SK-N-DZ, SK-N-AS, and SK-N-FI) developed tumors after sc inoculation. However, these sc tumors failed to develop radiologically-detectable bone metastases. Histological examination revealed no metastases to soft tissue organs and bones even at 12 weeks. Accordingly, we inoculated these NB cells into the left ventricle of the heart, which is a well-established technique to develop bone metastases [17]. Among three NB cell lines tested, only SK-N-AS cells reproducibly developed discernible osteolytic lesions in the limbs on X-ray over a period of 5–6 weeks (Fig. 1A). Some mice (~40%) showed hind limb paralysis with metastases to spine and spinal cord. Mice inoculated with SK-N-AS cells also demonstrated metastases to adrenal gland, kidney and lung but not liver, with a decrease in body weight, an average of 15.5% loss compared to control mice. Histological examination demonstrated extensive tumor colonization in the bone marrow cavity and destruction of trabecular bone (Fig. 1B). Increased numbers of TRAP (+) osteoclasts were observed along the endosteal bone surface (Fig. 1C). Blood Ca^{2+} concentration remained normal in mice received sc or heart injection of SK-N-AS cells (sc injection: 1.28 ± 0.06 mM, heart-injection: 1.26 ± 0.05 mM, control; 1.29 ± 0.03 mM, $n=5$). SK-N-A-DZ and SK-N-FI cells rarely developed bone metastases following heart inoculation.

3.2. TRAP (+) MNC formation in the co-cultures of NB cells with mouse BMCs

To determine the mechanism of increased osteoclasts in the bone metastases of SK-N-AS cells, we examined whether SK-N-AS cells supported osteoclast formation in the co-cultures with mouse BMCs. We found that TRAP (+) MNCs formed in the co-cultures of SK-N-AS cells and mouse BMCs (Fig. 2A and B). These TRAP (+) MNCs cells formed resorption pits on dentine slices (data not shown). In contrast, co-cultures of mouse BMCs with SK-N-DZ or SK-N-FI cells that failed to develop bone metastases showed no induction of osteoclastogenesis (Fig. 2A). Since receptor activator of NF-κB ligand (RANKL) expressed in marrow stromal cells plays a central role in osteoclastogenesis [25], we next examined whether SK-N-AS cells induced RANKL expression in mouse BMCs. RT-PCR analysis showed an induction of RANKL mRNA expression in mouse BMCs co-cultured with SK-N-AS cells (Fig. 2C). The

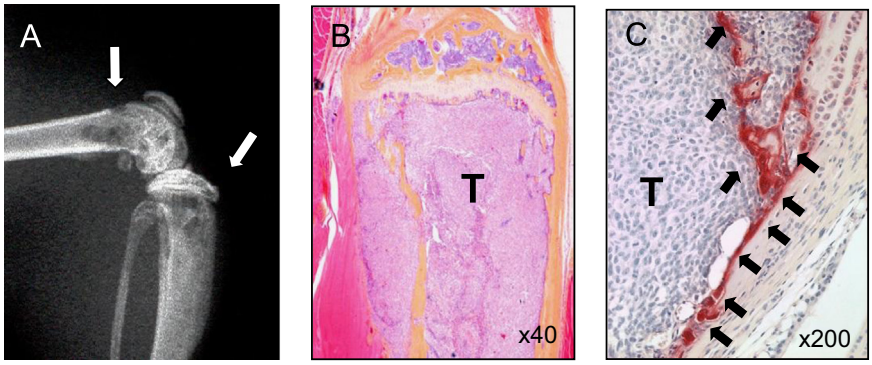

Fig. 1. Bone metastasis of the SK-N-AS human NB cell line. (A) Radiograph of hindlimbs of mouse bearing SK-N-AS tumors 40 days after intracardiac inoculation of 5×10^5 SK-N-AS tumor cells. Osteolytic bone metastases are indicated by arrows. (B) Histological pictures of bone metastases stained with H&E ($40 \times$). The bone marrow cavity was occupied by SK-N-AS tumor and trabecular bones were completely destroyed. (C) Histological pictures of bone metastases stained with TRAP ($200 \times$). Histological sections were made using proximal tibial midsection of mice bearing SK-N-AS cells. SK-N-AS tumor cells (T) extensively colonized bone marrow cavity with increased numbers of OCs (arrows) along the endosteal surface of bone.

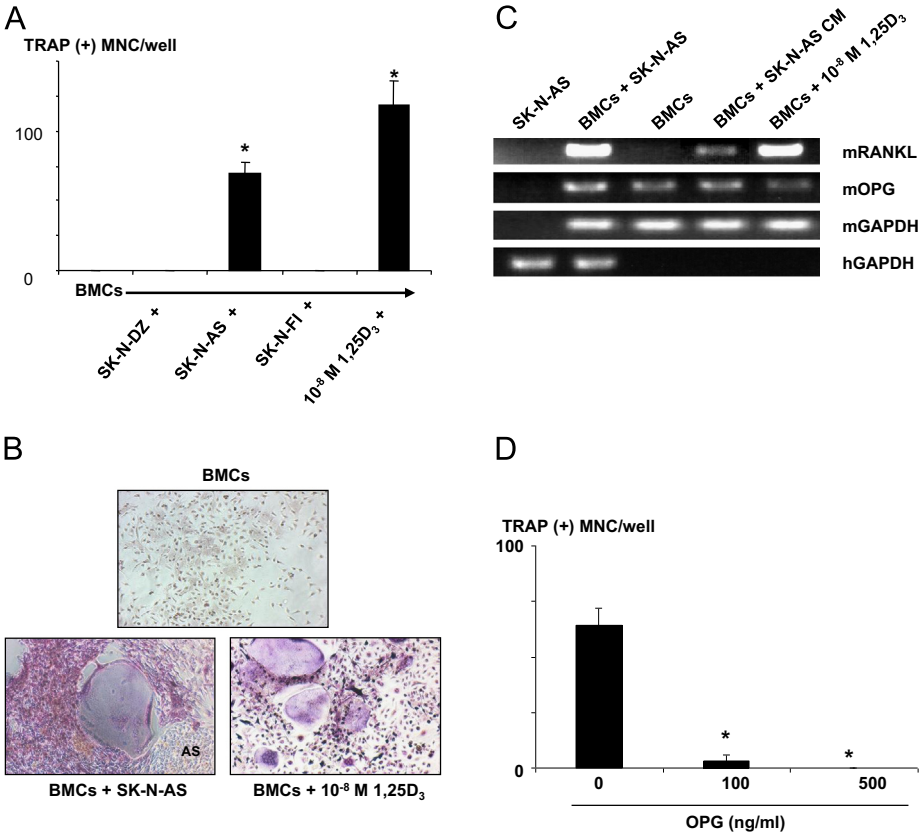

Fig. 2. TRAP (+) MNCs formation in the co-cultures of human NB cells and mouse BMCs. Mouse BMCs (5×10^5 cells/well) were co-cultured with or without (−) SK-N-DZ, SK-N-AS or SK-N-FI human NB cells (0.5×10^4 cells/well) without addition of osteoclastogenic cytokine for 6 days. $1,25D_3$ (10^{-8} M) served as positive control. (A) Formation of TRAP (+) MNCs. Data are expressed as mean ± SE ($n=3$). There was no TRAP (+) MNC formation in the cultures of BMCs alone and co-cultures of BMCs and SK-N-DZ or SK-N-FI cells in the absence of osteoclastogenic cytokine. In contrast, the co-cultures of BMCs and SK-N-AS cells produced TRAP (+) MNC in the absence of osteoclastogenic cytokine to an equivalent level to that of $1,25D_3$ (10^{-8} M). *Significantly different from SK-N-DZ and SK-N-FI ($p < 0.01$). (B) Representative pictures of TRAP (+) MNCs formed in the co-cultures of BMCs and SK-N-AS cells. (C) RT-PCR analysis of RANKL expression in mouse BMCs. Mouse BMCs (4×10^6 cells/well) were co-cultured with or without SK-N-AS cells (4×10^4 cells/well) or cultured in the presence of the conditioned medium from SK-N-AS cells (SK-N-AS CM, 20% v/v) for 6 days. Mouse BMCs co-cultured with SK-N-AS cells or treated with SK-N-AS CM showed increased mRANKL mRNA expression. mRANKL was undetectable in untreated BMCs. $1,25D_3$ served as positive control. (D) Effects of OPG on TRAP (+) MNC formation in the co-cultures of SK-N-AS cells and mouse BMCs. Mouse BMCs (5×10^5 cells/well) were co-cultured with SK-N-AS cells (0.5×10^4 cells/well) in the presence of OPG for 6 days and TRAP (+) MNCs were counted. OPG inhibited TRAP formation in mouse BM cells induced by SK-N-AS cells in a dose-dependent manner. Data are expressed as mean ± SE ($n=3$). *Significantly different from untreated group ($p < 0.01$).

conditioned medium (CM) harvested from SK-N-AS cells also induced mRANKL mRNA expression in mouse BMCs (Fig. 2C). Consistent with up-regulation of mRANKL in the co-cultures of mouse BMCs and SK-N-AS cells, osteoprotegerin (OPG), a natural antagonist of RANKL [25], reduced TRAP (+) MNC formation in the co-cultures in a dose-dependent manner (Fig. 2D). SK-N-AS cells did not change mRNA expression of OPG in mouse BMCs. These results collectively suggest that a soluble factor produced by SK-N-MS cells induces RANKL expression in mouse BMCs, leading to an induction of osteoclastogenesis.

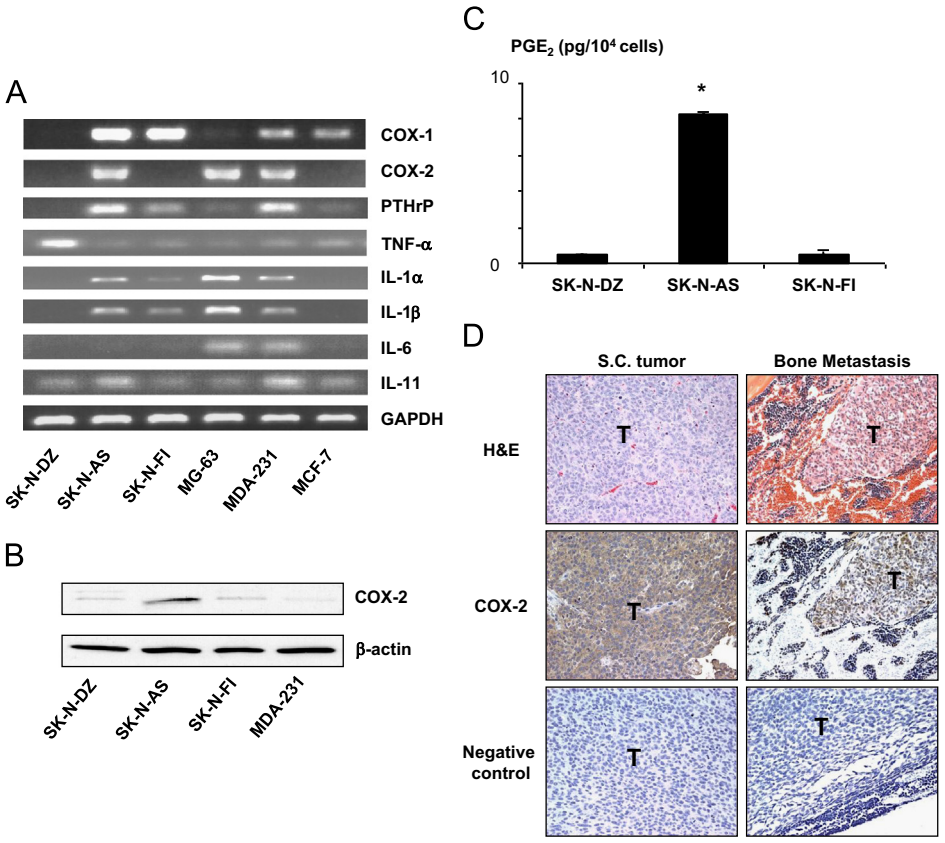

Fig. 3. (A) RT-PCR analysis of the expression of osteoclastogenic cytokine mRNA in SK-N-AS, SK-N-DZ, SK-N-FI human NB cells and a variety of human tumors. MG-63: human osteosarcoma cell line; MDA-231: estrogen-independent human breast cancer cell line; MCF-7: estrogen-dependent human breast cancer cell line. Note that COX-2 was expressed in SK-N-AS cells but not SK-N-DZ and SK-N-FI cells. (B) Western analysis of COX-2 expression in SK-N-AS, SK-N-DZ, SK-N-FI human NB cells. SK-N-AS cells showed strong COX-2 expression. (C): PGE_2 production in SK-N-AS, SK-N-DZ, SK-N-FI human NB cells in culture. Confluent cells were cultured in serum-free medium for 48 h and CMs were harvested and determined PGE2 concentrations using an EIA kit as described in the text. Data were normalized for cell number. Data are expressed as mean ± SE ($n=3$). *Significantly greater than SK-N-DZ and SK-N-FI cultures ($p<0.01$). (D): COX-2 expression in SK-N-AS tumor *in vivo*. Paraffin-embedded specimens from sc tumors and bone metastases of SK-N-AS were stained with H&E and anti-COX-2 antibody as described in the text. COX-2 expression was detected in both sc tumor and bone metastasis. T: tumor; Negative control: no primary antibody. Original magnification, 200 ×.

3.3. *Expression of COX-2 and PGE_2 production in SK-N-AS cells*

To search for a soluble factor responsible for the induction of osteoclastogenesis, we examined mRNA expression of several known osteoclastogenic cytokines in SK-N-AS cells by RT-PCR. As shown in Fig. 3A, SK-N-AS cells expressed mRNA of parathyroid hormone-related protein (PTH-rP), interleukin-1 α (IL-1α), IL-1β and IL-11 but not tumor necrosis factor α (TNFα) and IL-6. Of note, COX-2 mRNA expression was observed only in SK-N-AS cells in three human NB cell lines studied here. COX-2 is a rate-limiting enzyme in PG synthesis [26]. PGs, especially PGE_2, are known as potent osteoclastogenic factors [12]. Western analysis also showed that only SK-N-AS cells expressed COX-2 protein (Fig. 3B). Furthermore, EIA measurement demonstrated that SK-N-AS cells produced larger amounts of PGE_2 than SK-N-DZ and SK-N-FI cells (Fig. 3C). Immunohistochemical examination showed that sc tumor and bone metastases of SK-N-AS were positive for COX-2 (Fig. 3D). Taken together, these results suggest that PGE_2 produced by SK-N-AS cells plays a role in increased osteoclastogenesis in the co-cultures.

3.4. *Effect of indomethacin and NS-398 on TRAP (+) MNC formation in co-cultures*

To verify the role of COX-2/PGE_2 in the TRAP (+) MNC formation in the co-cultures, the effects of a non-selective COX inhibitor indomethacin and a selective COX-2 inhibitor NS-398 were examined. Both agents inhibited PGE_2 production (Fig. 4A) and TRAP (+) MNC formation (Fig. 4B and C) in the co-cultures. Addition of 10^{-6} M PGE_2 to the NS-398-treated co-cultures restored the TRAP (+) MNC formation, suggesting that the effects of NS-398 were not due to toxicity (data not shown).

3.5. *Effects of NS-398 on SK-N-AS bone metastasis*

Next, we examined whether COX-2 played a role in bone metastasis. As shown in Fig. 7A, control mice developed extensive osteolytic bone metastases 5 weeks after intracardiac inoculation of SK-N-AS cell inoculation. Treatment with NS-398 (15 mg/kg body weight) markedly reduced osteolytic lesions on radiographs (Figs. 5A and B; 4.12 ± 0.65 mm^2 (untreated) *vs* 1.53 ± 0.71 mm^2 (NS-398); $p<0.05$). The number of bone metastases also significantly reduced in NS-398-treated mice compared to untreated mice (Fig. 5C; 3.8 ± 0.2 (untreated) *vs* 1.8 ± 0.8 (NS-398); $p<0.05$). Histological examination revealed that NS-398 markedly reduced the number of OCs compared with untreated group (Fig. 5D). NS-398 also significantly prevented body weight loss in tumor-bearing mice (17.72 ± 0.82 g (untreated) *vs* 21.04 ± 0.82 g (NS-398); $p<0.05$).

3.6. *Effect of NS-398 on subcutaneous SK-N-AS tumor formation and angiogenesis*

We next investigated the effects of NS-398 on subcutaneous SK-N-AS tumor formation. Daily treatment with NS-398 (15 mg/kg

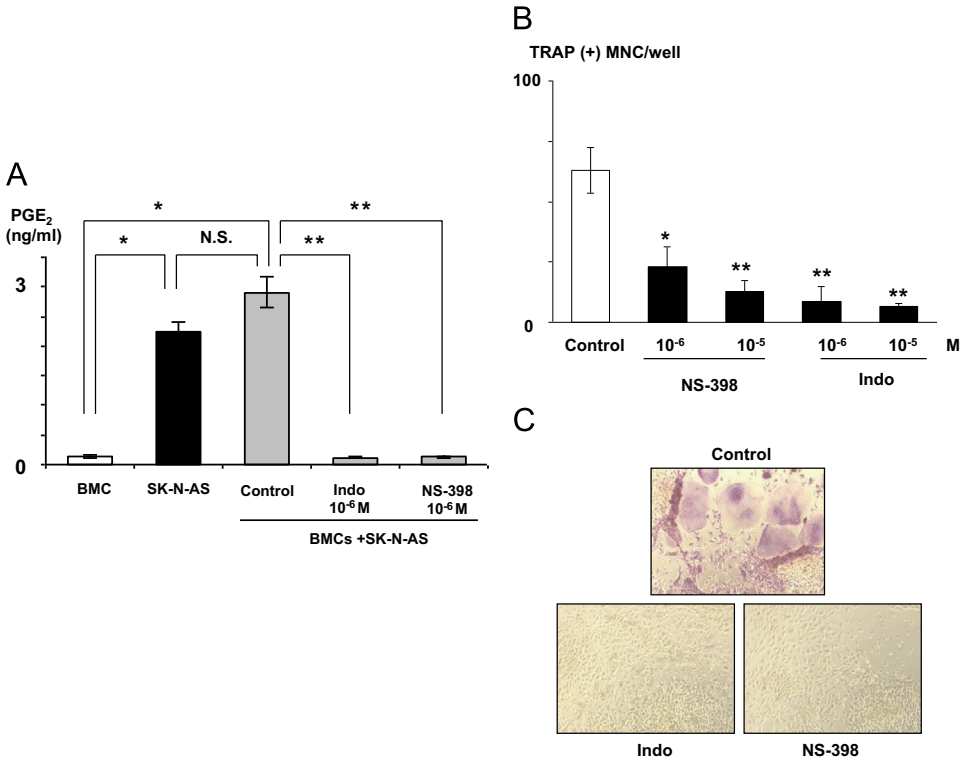

Fig. 4. (A) Effects of COX inhibitors on PGE_2 production in the co-cultures of mouse BMCs and SK-N-AS cells. Indomethacin (Indo) and NS-398 significantly suppressed PGE_2 production in the co-cultures. Mouse BMCs (5×10^5 cells/well) were co-cultured with SK-N-AS cells (0.5×10^4 cells/well) in the absence or presence of indomethacin (10^{-6} M) or NS-398 (10^{-6} M) for 6 days. At the end of the experiments, CM were harvested and measured for PGE_2 concentrations (A). Remaining adherent cells were then stained for TRAP (B). (B) Effects of COX inhibitors on TRAP (+) MNC formation in the co-cultures of mouse BMCs and SK-N-AS cells. Indomethacin and NS-398 inhibited PGE_2 production and TRAP (+) MNC formation in the co-cultures. Data are expressed as mean ± SE ($n=3$). *Significantly different from BMC ($p < 0.01$). **Significantly different from control ($p < 0.01$). (C) Representative pictures of TRAP (+) MNC formation in the co-cultures of mouse BMCs and SK-N-AS cells in the absence (top) or presence of indomethacin (bottom left) or NS-398 (bottom right).

body weight) significantly inhibited tumor enlargement as determined by volume (Fig. 6A). Average tumor wet weight at sacrifice was 9.44 ± 2.60 g in untreated mice and 1.22 ± 0.69 g in NS-398-treated mice (Fig. 6B). SK-N-AS cell proliferation in the subcutaneous tumor determined by immunohistochemical staining for PCNA was not apparently different between untreated and NS-398-treated tumors (data not shown). In addition, NS-398 had no effects on the cell proliferation of SK-N-AS cells in culture at concentrations as high as 200 μM assessed by MTT assay (data not shown). These results suggest that the inhibition of subcutaneous SK-N-AS tumor formation by NS-398 is not due to direct inhibition of SK-N-AS cell proliferation.

To investigate the mechanism by which NS-398 reduced tumor development independent of cell proliferation, we examined the effects of NS-398 on tumor-associated angiogenesis. Vascularization was identified by staining with an anti-factor VIII antibody. Representative sections from untreated and NS-398-treated tumors are shown in Fig. 6C. Blood vessels in the tumors of untreated mice showed intensive staining of factor VIII, indicating well-developed vascular networks. In contrast, there were few blood vessels in the tumors of NS-398-treated mice. To determine whether the inhibitory effects of NS-398 on the angiogenesis was due to the suppression of VEGF, a powerful stimulator of angiogenesis, the expression of VEGF-A was studied by immunohistochemistry. VEGF-A expression was reduced in NS-398-treated mice compared with untreated mice (Fig. 6C). RT-PCR displayed that NS-398 inhibited the expression of VEGF-A mRNA, in particular VEGF-A_{121} isoform in SK-N-AS tumor (Fig. 6D). We also found that SK-N-AS cells expressed PGE_2 receptors, EP1, EP2, EP3 and EP4 and PGE_2 increased VEGF mRNA expression by RT-PCR in SK-N-AS cells (data not shown). These results suggest that PGE_2 is an autocrine stimulator of angiogenesis via up-regulation of VEGF-A expression in SK-N-AS cells.

3.7. *Effects of NS-398 on SK-N-AS adrenal gland metastasis*

Since NB tumor arises in adrenal gland [1,2] and adrenal gland is one of the preferential sites of metastasis in the heart injection model [27], we next examined the effects of NS-398 on adrenal gland metastases of SK-N-AS cells following intracardiac inoculation. Although not statistically significant, NS-398 decreased the number of adrenal gland metastases (1.8 ± 0.2 (untreated) *vs* 1.0 ± 0.4 (NS-398)) on histological sections (Fig. 7A), while organ weight of adrenal gland including metastatic SK-N-AS tumors in NS-398-treated mice was significantly lesser than untreated mice (0.178 ± 0.064 g (untreated) *vs* 0.0482 ± 0.023 g (NS-398); $p < 0.05$) (Fig. 7B). These results suggest that NS-398 inhibited metastases not only to bone but also adrenal glands. Histological examination of gastric mucosa and liver showed no toxic effects of NS-398 in mice during the experiments.

3.8. *Contribution of PTH-rP to SK-N-AS bone metastasis*

PTH-rP is a potent osteoclastogenic factor and has long been implicated in breast cancer metastasis to bone [8,9]. SK-N-AS cells express PTH-rP mRNA. However, the levels of PTH-rP protein produced by SK-N-AS cells in culture were low compared with the MDA-MB-231 human breast cancer cells that cause extensive bone metastases (basal level: 0.51 ± 0.05 pmol/10^5 SK-N-AS cells *vs* 1.46 ± 0.14 pmol/10^5 MDA-MB-231 cells). TGFβ, which is a potent stimulator of PTH-rP production [8,9], did not increase PTH-rP production in SK-N-AS cells in culture (PTH-rP production

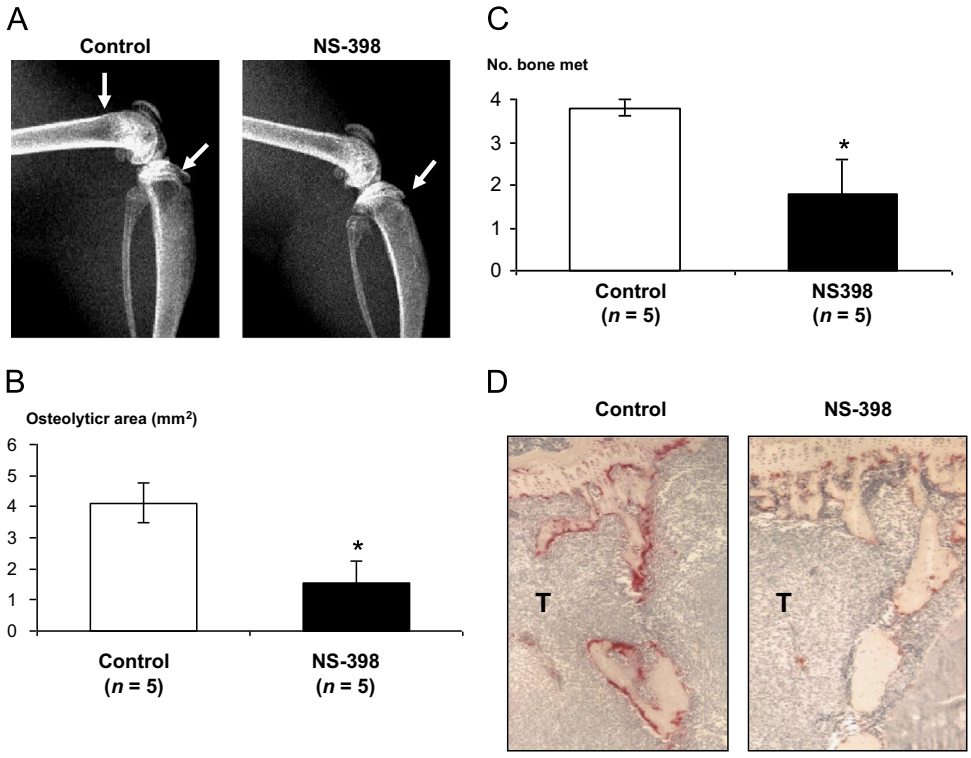

Fig. 5. Effects of NS-398 on SK-N-AS bone metastasis. Mice inoculated with SK-N-AS cells (5×10^5 cells) via the left cardiac ventricle were treated with either vehicle (control) or NS-398 (15 mg/kg. ip). Five weeks after tumor inoculation, radiographs were taken and bones were harvested for histological analyses. (A) Representative radiographs of hindlimbs of mice. Osteolytic lesions are indicated by *arrows*. (B) Quantitative measurement of the area of the osteolytic lesions on radiographs as assessed by computerized image analysis. MNS-398 significantly decreased osteolytic area on radiographs. Data are expressed as mean ± SE ($n=5$). *Significantly different from control ($p < 0.05$). (C): Number of osteolytic lesions in hindlimbs of mice on radiographs. Data are expressed as mean ± SE ($n=5$). *Significantly different from control ($p < 0.05$). (D): TRAP staining of the midtibial metaphysis of representative mice treated with either vehicle (control) or NS-398. In mice treated with NS-398, there were less TRAP (+) OCs along trabecular bone compared to control mice. T: tumor.

in the presence of 10 ng/ml TGFβ: 0.75 ± 0.04 pmol/10^5 SK-N-AS cells *vs* 3.84 ± 0.29 pmol/10^5 MDA-MB-231 cells). Furthermore, SK-N-FI cells that had no capacity to develop bone metastases following intracardiac inoculation also expressed PTH-rP mRNA by RT-PCR. Therefore, it is unlikely that PTH-rP contributes to the osteolytic bone metastases of SK-N-AS NB.

4. Discussion

In the present study, we have shown that, of the three human NB cell lines examined, only the SK-N-AS human NB cell line reproducibly developed radiologically and histologically discernible osteolytic bone metastases following intracardiac inoculation in nude mice. Histological examination demonstrated that there were numerous TRAP-positive osteoclasts present along the endosteal surface of eroded bone in the SK-N-AS bone metastases. In the co-cultures with mouse BMCs, SK-N-AS cells induced TRAP (+) MNC formation in the absence of osteoclastogenic factor. The induction was RANKL-dependent, since mRANKL mRNA expression was induced in mouse BMCs and TRAP (+) MNC formation was decreased by OPG in the co-culture with SK-NAS cells. On the other hand, SK-N-DZ and SK-N-FI cells that failed to develop bone metastases did not induce TRAP (+) MNC formation in the co-cultures with mouse BMCs. These results suggest that SK-N-AS cells possess the capacity to cause osteolytic bone metastases accompanied with RANKL-dependent osteoclastogenesis. Subsequently, we attempted to understand this capacity at molecular levels. The result that SK-N-AS CM increased TRAP (+) MNC formation in mouse BMCs suggests that SK-N-AS cells produce a soluble osteoclastogenic factor. We found that SK-N-AS cells strongly expressed COX-2 and produced substantial levels of PGE_2, while non-bone metastatic SK-N-DZ and SK-N-FI cells did not express COX-2 and produced little PGE_2. Furthermore, the selective COX-2 inhibitor NS-398 significantly reduced bone metastases and osteoclastogenesis *in vivo* and *in vitro*. Taken together, these experimental data suggest that COX-2 expression and consequent PGE_2 production are responsible for causing bone metastases with increased osteoclastogenesis in SK-N-AS human NB cells. Consistent with our results, it was reported that elevated COX-2 expression and PGE_2 production and induction of apoptosis and inhibition of tumor growth *in vivo* by the nonsteroidal anti-inflammatory drugs in NB [28,29]. Thus, we show here an establishment of a reproducible animal model of osteolytic bone metastases of human NB in which COX-2/PGE_2 plays a critical role. We believe that this model leads us to deepen our understanding of the mechanism of bone metastasis of NB.

The animal model described here is also expected to lead us to design mechanism-based therapeutic interventions for bone metastases of NB. In this context, it is notable that the selective COX-2 inhibitor NS-398, which is known to selectively inhibit COX-2 without affecting COX-1 activity [30], inhibited bone metastases of SK-N-AS cells. Consistent with the results described here, we reported that NS-398 significantly reduced osteolytic bone metastases of MDA-MB-231 human breast cancer cells [12]. Moreover, Sabino et al. [31] described that NS-398 not only decreased 2472 sarcoma colonization in bone and bone destruction but also bone pain associated with tumor growth, suggesting an additional potential beneficial effect of COX-2 inhibitors for NB treatment. Bone pain is one of the most common and devastating complications in bone metastases in children with NB [32]. Another notable finding in our study is that NS-398 inhibited

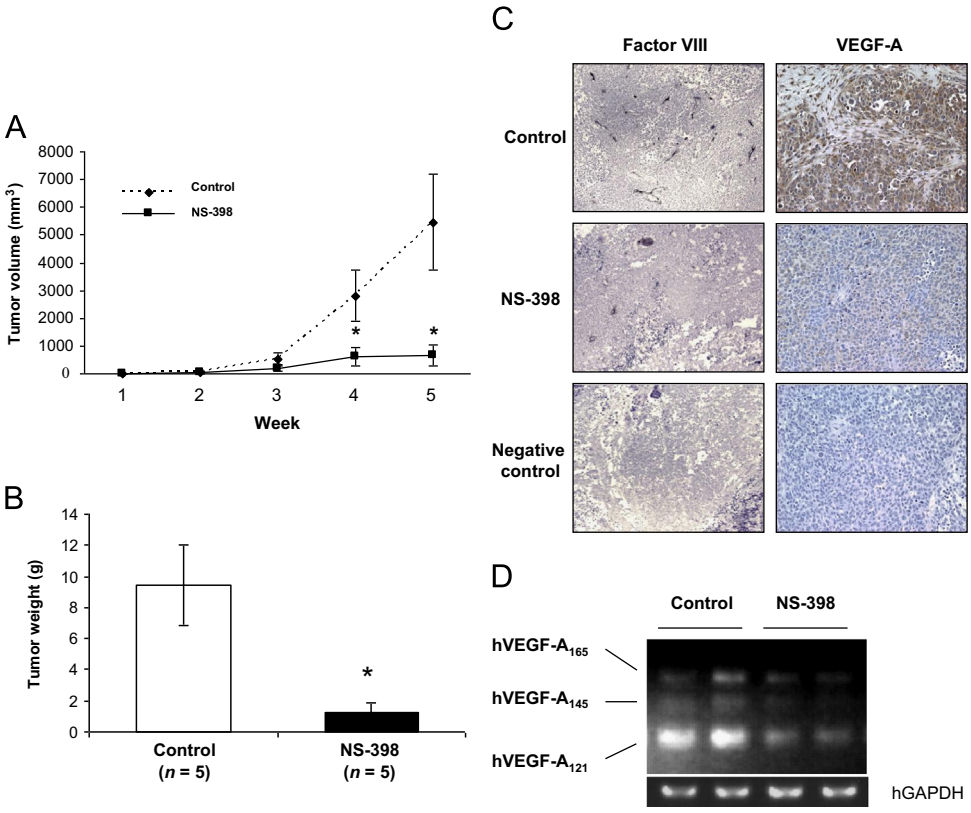

Fig. 6. Effects of NS-398 on subcutaneous SK-N-AS tumor development. Three days after sc inoculation of SK-N-AS cells (2.5×10^6 cells), mice received daily injections of NS-398 (15 mg/kg, ip) or vehicle (control) for the following 5 weeks ($n=5$ for each group). (A): Development of sc SK-N-AS tumors. Data are expressed as mean ± SE ($n=5$). *Significantly different from control ($p < 0.05$). (B) Tumor wet weight at 5 weeks after sc inoculation. Treatment with NS-398 significantly inhibited tumor wet weight. Data are expressed as mean ± SE ($n=5$). *Significantly different from control ($p < 0.05$). (C) Immunohistochemical examination of subcutaneous SK-N-AS tumors. Tumor sections were stained with anti-factor VIII antibody and anti-VEGF-A antibody as described in Materials and Methods. Tumors from NS-398-treated mice showed a decrease in microvessel density (factor VIII staining) and reduced intensity of VEGF-A staining compared to control. Negative control: no primary antibody. Original magnification, x50 (factor VIII); x200 (VEGF-A). (D) Effects of NS-398 on VEGF-A mRNA expression in SK-N-AS tumor *in vivo*. One μg of total RNA from sc tumors was subjected to RT-PCR analysis in duplicate. NS-398 down-regulated hVEGF-A_{121} mRNA.

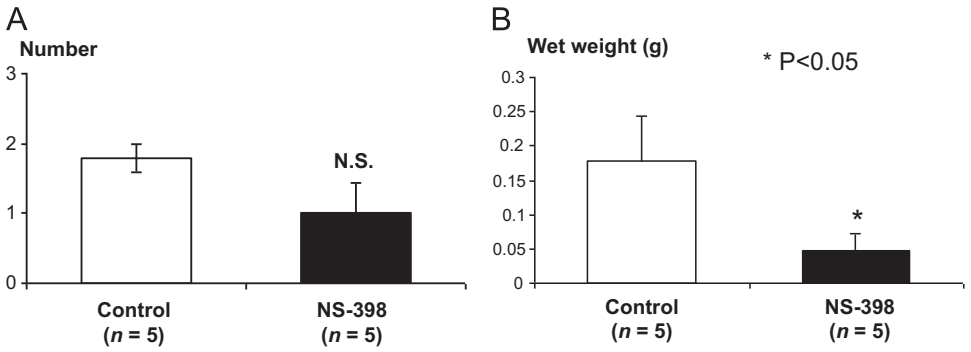

Fig. 7. Effects of NS-398 on SK-N-AS adrenal gland metastasis. Mice inoculated with SK-N-AS cells (5×10^5 cells) via the left cardiac ventricle were treated as described in Fig. 7. Five weeks after tumor inoculation, adrenal glands with metastases were excised, wet weight was measured and examined for the number of metastatic foci under dissecting microscope. SN-N-AS metastases were verified by histological examination. (A) Number of adrenal gland metastases. Data are expressed as mean ± SE ($n=5$). (B) Wet weight of adrenal gland with metastases. Data are expressed as mean ± SE ($n=5$). *Significantly different from control ($p < 0.05$).

not only bone metastases but also adrenal metastases. Adrenal gland is a preferential site for NB to initiate and expand, which leads to death [1,2]. Thus, selective COX-2 inhibitors may have beneficial effects on not only quality of life but survival in infants with NB. Clinical studies also reported that the selective COX-2 inhibitor celecoxib prevented the occurrence of colorectal adenomas [33] and showed some therapeutic effects in patients with breast [34], head and neck [35], cervical [36], non-small cell lung [37], colorectal [38] and ovarian cancer [39]. Of note, a recent clinical study described that oral celecoxib prevented the progression of neuroblastoma [40]. Further experimental and clinical studies are needed to verify the beneficial effects of selective COX-2 inhibitors for the treatment of infants with NB. The NB model described here would provide with a suitable preclinical model to conduct these studies.

Since the selective COX-2 inhibitor NS-398 did not inhibit the proliferation of SK-N-AS cells *in vivo* and *in vitro*, we reasoned that the agent suppressed tumor-associated angiogenesis. Angiogenesis is essential for tumor cells to initiate, grow, survive, invade and spread [41]. VEGF, a specific mitogen for neovascularization, is a major factor in the promotion of tumor angiogenesis and growth of human cancers [42]. The importance of VEGF expression

associated with angiogenesis in tumor behavior is also suggested in NB [43]. Several recent experimental studies have reported that COX-2 inhibitors inhibit tumor angiogenesis through down-regulation of VEGF expression, thereby suppressing tumor growth in breast [44], colorectal [45] and pancreatic cancer [46]. Furthermore, it has been shown that celecoxib combined with irinotecan inhibits the growth of neuroblastoma xenografts through induction of apoptosis and suppression of angiogenesis with decreased VEGF expression [47]. Consistent with these previous studies, we found that NS-398 decreased vascularization and VEGF-A expression in subcutaneous SK-N-AS tumors. COX-2/PGE_2 is a well-known stimulator of angiogenesis [44–46]. Collectively, these results suggest that the inhibition by NS-398 of subcutaneous tumor growth and bone metastases of SK-N-AS NB is due to the suppression of VEGF and angiogenesis.

Based on the pathophysiology bone metastasis [8,9], inhibition of osteoclastic bone resorption is a mechanism-based treatment for bone metastases regardless of cancer type. Bisphosphonates (BPs), which are potent and specific inhibitors of osteoclastic bone resorption, have been widely used for the treatment of bone metastases [48]. An experimental animal study reported that the BP ibandronate inhibited osteolytic bone lesions developed after intra-femoral injection of NB cells [49]. However, caution is required for the use of BPs for the treatment of bone metastases of NB children, since administration of BP may have adverse effects on skeletal growth in growing infants [50]. In this context, COX-2 inhibitors could be an alternative agent in the management of bone metastases in infants with NB with less adverse effects on skeletal growth.

In summary, we have established an animal model of human NB bone metastasis in which COX-2/PGE_2 plays a critical role. We provide pre-clinical data supporting the use of COX-2 inhibitors in the treatment of bone metastases in NB.

Conflict of interest statement

The authors declare that there are no conflicts of interest.

Acknowledgment

This study was supported by NIH Grant RO1 CA103034-01 (TY) and grants-in-aid 11557136 (TY), 17014058 (TY) and 21st Century Center of Excellence Program (12137205, TY) from the Ministry of Education, Culture, Sports, Science and Technology, Japan.

References

[1] Brodeur GM. Neuroblastoma: biological insights into a clinical enigma. Nat Rev Cancer 2003;3:203–16.
[2] Maris JM. Recent advances in neuroblastoma. N Engl J Med 2010;362:2202–11.
[3] DuBois SG, Kalika Y, Lukens JN, Brodeur GM, Seeger RC, Atkinson JB, Haase GM, Black CT, Perez C, Shimada H, Gerbing R, Stram DO, Matthay KK. Metastatic sites in stage IV and IVS neuroblastoma correlate with age, tumor biology, and survival. J Pediatr Hematol Oncol 1999;21:181–9.
[4] Granchi D, Corrias MV, Garaventa A, Baglìo SR, Cangemi G, Carlini B, Paolucci P, Giunti A, Baldini N. Neuroblastoma and bone metastases: clinical significance and prognostic value of Dickkopf 1 plasma levels. Bone 2011;48:152–9.
[5] Matthay KK, Villablanca JG, Seeger RC, Stram DO, Harris RE, Ramsay NK, Swift P, Shimada H, Black CT, Brodeur GM, Gerbing RB, Reynolds CP. Treatment of high-risk neuroblastoma with intensive chemotherapy, radiotherapy, autologous bone marrow transplantation, and 13-cis-retinoic acid. Children's Cancer Group. N Engl J Med 1999;341:1165–73.
[6] Hero B, Simon T, Horz S, Berthold F. Metastatic neuroblastoma in infancy: what does the pattern of metastases contribute to prognosis? Med Pediatr Oncol 2000;35:683–7.
[7] Ladenstein R, Philip T, Lasset C, Hartmann O, Garaventa A, Pinkerton R, Michon J, Pritchard J, Klingebiel T, Kremens B, Pearson A, Coze C, Paolucci P, Frappaz D, Gadner H, Chauvin F. Multivariate analysis of risk factors in stage 4 neuroblastoma patients over the age of one year treated with megatherapy and stem-cell transplantation: a report from the European Bone Marrow Transplantation Solid Tumor Registry. J Clin Oncol 1998;16:953–65.
[8] Yoneda T, Hiraga T. Crosstalk between cancer cells and bone microenvironment in bone metastasis. Biochem Biophys Res Commun 2005;328:679–87.
[9] Weilbaecher KN, Guise TA, McCauley LK. Cancer to bone: a fatal attraction. Nat Rev Cancer 2011;11:411–25.
[10] Hiraga T, Myoui A, Hashimoto N, Sasaki A, Hata K, Morita Y, Yoshikawa H, Rosen CJ, Mundy GR, Yoneda T. Bone-derived IGF mediates crosstalk between bone and breast cancer cells in bony metastases. Cancer Res 2012;72:4238–49.
[11] Yin JJ, Selander K, Chirgwin JM, Dallas M, Grubbs BG, Wieser R, Massagué J, Mundy GR, Guise TA. TGFβ signaling blockade inhibits PTH-rP secretion by breast cancer cells and bone metastases development. J Clin Invest 1999;103:197–206.
[12] Hiraga T, Myoui A, Choi ME, Yoshikawa H, Yoneda T. Stimulation of cyclooxygenase-2 expression by bone-derived transforming growth factor β enhances bone metastases in breast cancer. Cancer Res 2006;66:2067–73.
[13] Sohara Y, Shimada H, DeClerck YA. Mechanisms of bone invasion and metastasis in human neuroblastoma. Cancer Lett 2005;228:203–9.
[14] Michigami T, Ihara-Watanabe M, Yamazaki M, Ozono K. Receptor activator of nuclear factor kappaB ligand (RANKL) is a key molecule of osteoclast formation for bone metastasis in a newly developed model of human neuroblastoma. Cancer Res 2001;61:1637–44.
[15] Granchi D, Garaventa A, Amato I, Paolucci P, Baldini N. Plasma levels of receptor activator of nuclear factor-kappaB ligand and osteoprotegerin in patients with neuroblastoma. Int J Cancer 2006;119:146–51.
[16] van Golen CM, Schwab TS, Kim B, Soules ME, Su Oh S, Fung K, van Golen KL, Feldman EL. Insulin-like growth factor-I receptor expression regulates neuroblastoma metastasis to bone. Cancer Res 2006;66:6570–8.
[17] Sasaki A, Boyce BF, Story B, Wright KR, Chapman M, Boyce R, Mundy GR, Yoneda T. Bisphosphonate risedronate reduces metastatic human breast cancer burden in bone in nude mice. Cancer Res 1995;55:3551–7.
[18] Yoneda T, Lowe C, Lee CH, Gutierrez G, Niewolna M, Williams PJ, Izbicka E, Uehara Y, Mundy GR. Herbimycin A a $pp60^{c\text{-}src}$ tyrosine kinase inhibitor, inhibits osteoclastic bone resorption *in vitro* and hypercalcemia *in vivo*. J Clin Invest 1993;91:2791–5.
[19] Takahashi N, Yamana H, Yoshiki S, Roodman GD, Mundy GR, Jones SJ, Boyde A, Suda T. Osteoclast-like cell formation and its regulation by osteotropic hormones in mouse bone marrow cultures. Endocrinology 1988;122:1373–82.
[20] Udagawa N, Takahashi N, Akatsu T, Sasaki T, Yamaguchi A, Kodama H, Martin TJ, Suda T. The bone marrow-derived stromal cell lines MC3T3-G2/PA6 and ST2 support osteoclast-like cell differentiation in cocultures with mouse spleen cells. Endocrinology 1989;125:1805–13.
[21] Thomas RJ, Guise TA, Yin JJ, Elliott J, Horwood NJ, Martin TJ, Gillespie MT. Breast cancer cells interact with osteoblasts to support osteoclast formation. Endocrinology 1999;140:4451–8.
[22] Souza RF, Shewmake K, Beer DG, Cryer B, Spechler SJ. Selective inhibition of cyclooxygenase-2 suppresses growth and induces apoptosis in human esophageal adenocarcinoma cells. Cancer Res 2000;60:5767–72.
[23] Ohshiba T, Miyaura C, Ito A. Role of prostaglandin E produced by osteoblasts in osteolysis due to bone metastasis. Biochem Biophys Res Commun 2003;300:957–64.
[24] Abdel-Majid RM, Marshall JS. Prostaglandin E_2 induces degranulation-independent production of vascular endothelial growth factor by human mast cells. J Immunol 2004;172:1227–36.
[25] Lacey DL, Boyle WJ, Simonet WS, Kostenuik PJ, Dougall WC, Sullivan JK, San Martin J, Dansey R. Bench to bedside: elucidation of the OPG–RANK–RANKL pathway and the development of denosumab. Nat Rev Drug Discov 2012;11:401–19.
[26] Menter DG, Schilsky RL, DuBois RN. Cyclooxygenase-2 and cancer treatment: understanding the risk should be worth the reward. Clin Cancer Res 2010;16:1384–90.
[27] Michigami T, Hiraga T, Williams PJ, Niewolna M, Nishimura R, Mundy GR, Yoneda T. The effect of the bisphosphonate ibandronate on breast cancer metastasis to visceral organs. Breast Cancer Res Treat 2002;75:249–58.
[28] Johnsen JI, Lindskog M, Ponthan F, Pettersen I, Elfman L, Orrego A, Sveinbjörnsson B, Kogner P. Cyclooxygenase-2 is expressed in neuroblastoma, and nonsteroidal anti-inflammatory drugs induce apoptosis and inhibit tumor growth *in vivo*. Cancer Res 2004;64:7210–5.
[29] Rasmuson A, Kock A, Fuskevåg OM, Kruspig B, Simón-Santamaría J, Gogvadze V, Johnsen JI, Kogner P, Sveinbjörnsson B. Autocrine prostaglandin E_2 signaling promotes tumor cell survival and proliferation in childhood neuroblastoma. PLoS One 2012;7:e29331.
[30] Nakano M, Denda N, Matsumoto M, Kawamura M, Kawakubo Y, Hatanaka K, Hiramoto Y, Sato Y, Noshiro M, Harada Y. Interaction between cyclooxygenase (COX)-1- and COX-2-products modulates COX-2 expression in the late phase of acute inflammation. Eur J Pharmacol 2007;559:210–8.
[31] Sabino MA, Ghilardi JR, Jongen JL, Keyser CP, Luger NM, Mach DB, Peters CM, Rogers SD, Schwei MJ, de Felipe C, Mantyh PW. Simultaneous reduction in cancer pain, bone destruction, and tumor growth by selective inhibition of cyclooxygenase-2. Cancer Res 2002;62:7343–9.
[32] Paulino AC. Palliative radiotherapy in children with neuroblastoma. Pediatr Hematol Oncol 2000;20:111–7.
[33] Arber N, Eagle CJ, Spicak J, Rácz I, Dite P, Hajer J, Zavoral M, Lechuga MJ, Gerletti P, Tang J, Rosenstein RB, Macdonald K, Bhadra P, Fowler R, Wittes J, Zauber AG, Solomon SD, Levin B, PreSAP Trial Investigators. Celecoxib for the prevention of colorectal adenomatous polyps. N Engl J Med 2006;355:885–95.

[34] Perroud HA, Rico MJ, Alasino CM, Queralt F, Mainetti LE, Pezzotto SM, Rozados VR, Scharovsky OG. Safety and therapeutic effect of metronomic chemotherapy with cyclophosphamide and celecoxib in advanced breast cancer patients. Future Oncol 2013;9:451–62.
[35] Shin DM, Zhang H, Saba NF, Chen AY, Nannapaneni S, Amin AR, Müller S, Lewis M, Sica G, Kono S, Brandes JC, Grist WJ, Moreno-Williams R, Beitler JJ, Thomas SM, Chen Z, Shin HJ, Grandis JR, Khuri FR, Chen ZG. Chemoprevention of head and neck cancer by simultaneous blocking of epidermal growth factor receptor and cyclooxygenase-2 signaling pathways: preclinical and clinical studies. Clin Cancer Res. 2013;19:1244–56.
[36] Doll CM, Winter K, Gaffney DK, Ryu JK, Jhingran A, Dicker AP, Weidhaas JB, Miller BE, Magliocco AM. COX-2 expression and survival in patients with locally advanced cervical cancer treated with chemoradiotherapy and celecoxib: a quantitative immunohistochemical analysis of RTOG C0128. Int J Gynecol Cancer 2013;23:176–83.
[37] Sörenson S, Fohlin H, Lindgren A, Lindskog M, Bergman B, Sederholm C, Ek L, Lamberg K, Clinchy B. Predictive role of plasma vascular endothelial growth factor for the effect of celecoxib in advanced non-small cell lung cancer treated with chemotherapy. Eur J Cancer 2013;49:115–20.
[38] Almhanna K, El-Rayes B, Sethi S, Dyson G, Heilbrun L, Philip PA, Sarkar F. Association between COX-2 expression and effectiveness of COX-2 inhibitors in a phase II trial in patients with metastatic colorectal adenocarcinoma. Anticancer Res 2012;32:3559–63.
[39] Reyners AK, de Munck L, Erdkamp FL, Smit WM, Hoekman K, Lalisang RI, de Graaf H, Wymenga AN, Polee M, Hollema H, van Vugt MA, Schaapveld M, Willemse PH, DoCaCel Study Group. A randomized phase II study investigating the addition of the specific COX-2 inhibitor celecoxib to docetaxel plus carboplatin as first-line chemotherapy for stage IC to IV epithelial ovarian cancer, Fallopian tube or primary peritoneal carcinomas: the DoCaCel study. Ann Oncol 2012;23:2896–902.
[40] Robison NJ, Campigotto F, Chi SN, Manley PE, Turner CD, Zimmerman MA, Chordas CA, Werger AM, Allen JC, Goldman S, Rubin JB, Isakoff MS, Pan WJ, Khatib DS, Comito MA, Bendel AE, Pietrantonio JB, Kondrat L, Hubbs SM, Neuberg DS, Kieran MW. A phase II trial of a multi-agent oral antiangiogenic (metronomic) regimen in children with recurrent or progressive cancer. Pediatr Blood Cancer 2014;61:636–42.
[41] Hanahan D, Weinberg RA. Hallmarks of cancer: the next generation. Cell 2011;144:646–74.
[42] Mittal K, Ebos J, Rini B. Angiogenesis and the tumor microenvironment: vascular endothelial growth factor and beyond. Semin Oncol 2014;41:235–51.
[43] Shusterman S, Maris JM. Prospects for therapeutic inhibition of neuroblastoma angiogenesis. Cancer Lett 2005;228:171–9.
[44] Xin X, Majumder M, Girish GV, Mohindra V, Maruyama T, Lala PK. Targeting COX-2 and EP4 to control tumor growth, angiogenesis, lymphangiogenesis and metastasis to the lungs and lymph nodes in a breast cancer model. Lab Invest. 2012;92:1115–28.
[45] Ninomiya I, Nagai N, Oyama K, Hayashi H, Tajima H, Kitagawa H, Fushida S, Fujimura T, Ohta T. Antitumor and anti-metastatic effects of cyclooxygenase-2 inhibition by celecoxib on human colorectal carcinoma xenografts in nude mouse rectum. Oncol Rep 2012;28:777–84.
[46] Mayorek N, Naftali-Shani N, Grunewald M. Diclofenac inhibits tumor growth in a murine model of pancreatic cancer by modulation of VEGF levels and arginase activity. PLoS One 2010;5:e12715.
[47] Kaneko M, Kaneko S, Suzuki K. Prolonged low-dose administration of the cyclooxygenase-2 inhibitor celecoxib enhances the antitumor activity of irinotecan against neuroblastoma xenografts. Cancer Sci 2009;100:2193–201.
[48] Coleman R, Gnant M, Morgan G, Clezardin P. Effects of bone-targeted agents on cancer progression and mortality. J Natl Cancer Inst 2012;104:1059–67.
[49] Sohara Y, Shimada H, Scadeng M, Pollack H, Yamada S, Ye W, Reynolds CP, DeClerck YA. Lytic bone lesions in human neuroblastoma xenograft involve osteoclast recruitment and are inhibited by bisphosphonate. Cancer Res 2003;63:3026–31.
[50] Whyte MP, Wenkert D, Clements KL, McAlister WH, Mumm S. Bisphosphonate-induced osteopetrosis. N Engl J Med 2003;349:457–63.